J. Fluid Mech. (2012), *vol.* 703, *pp.* 391–401.
doi:10.1017/jfm.2012.237

Analytically approximate natural sloshing modes for a spherical tank shape

Odd M. Faltinsen† and Alexander N. Timokha

Centre for Ships and Ocean Structures & Department of Marine Technology, Norwegian University of Science and Technology, NO-7091, Trondheim, Norway

(Received 29 February 2012; revised 10 April 2012; accepted 16 May 2012; first published online 12 June 2012)

The multimodal method requires analytical (exact or approximate) natural sloshing modes that exactly satisfy the Laplace equation and boundary condition on the wetted tank surface. When dealing with the nonlinear sloshing problem, the modes should also allow for an analytical continuation throughout the mean free surface. Appropriate analytically approximate modes were constructed by Faltinsen & Timokha (*J. Fluid Mech.*, vol. 695, 2012, pp. 467–477) for the two-dimensional circular tank. The present paper extends this result to the three-dimensional, spherical tank shape and, based on that, establishes specific properties of the linear liquid sloshing.

Key words: computational methods, variational methods, wave–structure interactions

1. Introduction

Sloshing in spherical tanks is, for instance, of concern for liquefied natural gas (LNG) carriers (Faltinsen & Timokha 2009, chap. 1) and water supply towers (Curadelli *et al.* 2010). The hydrodynamic response (resulting forces and moments) due to sloshing in spherical tanks may be described numerically by computational fluid dynamics (Faltinsen & Timokha 2009; Rebouillat & Liksonov 2010), or analytically by the multimodal method (Faltinsen & Timokha 2009, chaps. 5, 7–9). The multimodal method makes it possible to derive a low-dimensional (modal) system of ordinary differential equations with respect to generalized coordinates responsible for amplification of natural sloshing modes.

Specifically, the multimodal method needs either exact or special approximate analytical sloshing modes which exactly satisfy both the Laplace equation and the boundary condition on the wetted tank surface. For nonlinear effects, the natural sloshing modes should be analytically expandable above the mean free surface. Even though the literature exemplifies various approximate methods for solving the natural sloshing problem, starting with famous works by Budiansky (1958, 1960), McIver (1989) and, recently, by Patkas & Karamanos (2007) and Drodos, Dimas & Karabalis (2008) and Karamanos, Papaprokopiou & Platyrrachos (2006, 2009), it is questionable whether all existing approximate natural sloshing modes can be adopted by the multimodal method due to the aforementioned specific requirements.

Appropriate approximate natural sloshing modes can be obtained by the Trefftz method employing a harmonic basis that exactly satisfies the zero-Neumann condition on the wetted tank surface. Such functional bases were constructed by Faltinsen &

† Email address for correspondence: oddfal@marin.ntnu.no

Timokha (2010) for the two-dimensional (circular) tank and Barnyak *et al.* (2011) for the three-dimensional (spherical) tank. They satisfy the zero-Neumann condition for any liquid fillings but possess a singular behaviour at the tank top. However, when the depth-to-tank-radius ratios were in the range $1.2 \lesssim h/R_0 < 2$, the Trefftz solution based on these harmonic bases was not sufficiently accurate.

The aforementioned failure can be explained by a specific asymptotic behaviour of the velocity potential at the contact line (the intersection of the mean free surface and the tank surface) causing, in particular, the 'high spot' results by Kulczycki & Kuznetsov (2011). The asymptotic behaviour was described by Komarenko (1980) (two-dimensional statement), Lukovsky, Barnyak & Komarenko (1984) (two-dimensional and axisymmetric three-dimensional tanks) and Komarenko (1998) (the three-dimensional axisymmetric tank, and accounting for the surface tension). To derive asymptotic terms possessing this asymptotic behaviour, Komarenko employed the procedure of Kondratiev (1967) by introducing an auxiliary two-dimensional boundary value problem formulated at the contact line. For the two-dimensional spectral sloshing problem with the Laplace equation, this auxiliary problem also deals with the Laplace equation and, as a consequence, Kondratiev's procedure yields two-dimensional harmonic functions possessing the corner-point asymptotic behaviour. However, these harmonic functions do not necessarily satisfy the zero-Neumann condition on the whole wetted tank wall. Normally, one should combine the asymptotic results by Komarenko (1980) with the conformal mapping technique to construct the required harmonic functions which satisfy, in addition, the tank surface condition. An example is given by Faltinsen & Timokha (2010) for a two-dimensional circular tank. For the three-dimensional spectral sloshing problem in an axisymmetric tank, Lukovsky *et al.* (1984) and Komarenko (1998) considered a family of two-dimensional spectral boundary problems in meridional cross-section appearing after separation of the angular coordinate in a cylindrical coordinate system (see (2.3)–(2.4)). The aforementioned two-dimensional auxiliary boundary problem is also formulated in the meridional plane. However, the asymptotic terms derived from the auxiliary problem possess the asymptotic behaviour of the natural sloshing modes, but, generally, do not return the three-dimensional harmonic functions and do not satisfy the tank surface (zero-Neumann) condition on the entire wetted wall.

For a two-dimensional circular shape, Faltinsen & Timokha (2010) employed the constructed set of harmonic functions capturing the required asymptotic behaviour and satisfying the zero Neumann condition on the wetted wall as 'correcting' functions in the Trefftz method. This procedure improved the convergence for the higher liquid filling ratios. Because the derived asymptotic terms by Lukovsky *et al.* (1984), generally speaking, do not satisfy the three-dimensional Laplace equation in the spherical domain and the zero-Neumann condition on the wetted tank surface, the authors' efforts to extend results by Faltinsen & Timokha (2010) to the three-dimensional spherical shape were not successful. An alternative approach is needed. Such an approach was proposed by Faltinsen & Timokha (2012) for a circular tank by studying an analytical continuation of the natural sloshing modes into the whole tank domain via a modified Poisson integral (see Polyanin 2001, § 7.1.2-3). The present paper shows how to generalize this approach to the spherical tank shape.

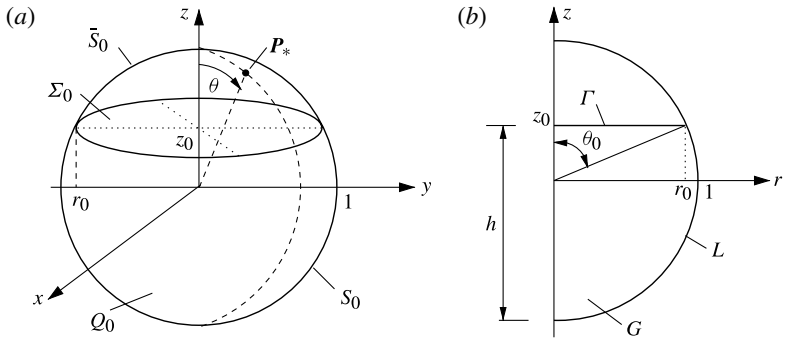

FIGURE 1. Geometric notation for the spectral boundary problems (2.1) and (2.3).

2. Theory

2.1. *Statement of the problem*

Henceforth, we consider a non-dimensional sloshing problem based on the characteristic size R_0 (radius) and time $\sqrt{R_0/g}$ (g is the acceleration due to gravity). This implies, in particular, that the spherical tank studied has unit radius and all the length dimensions introduced in figure 1 are scaled by R_0. The natural sloshing modes are the eigenfunctions φ_I of the spectral boundary problem (well known from surface wave theory: see Lamb 1932, chap. 10):

$$\nabla^2\varphi_I = 0 \quad \text{in } Q_0, \qquad \frac{\partial\varphi_I}{\partial n} = \kappa_I\varphi_I \quad \text{on } \Sigma_0, \qquad \frac{\partial\varphi_I}{\partial n} = 0 \quad \text{on } S_0, \qquad \int_{\Sigma_0}\varphi_I\,\mathrm{d}S = 0. \tag{2.1}$$

Here, Q_0 is the unperturbed liquid domain, S_0 is the wetted tank surface, Σ_0 is the mean free surface, and $\kappa_I > 0$ are the eigenvalues that define the non-dimensional natural sloshing frequencies, $\sigma_I = \sqrt{\kappa_I}$ (dimensional natural sloshing frequencies are $\bar{\sigma}_I = \sigma_I\sqrt{g/R_0}$). The spectral boundary problem (2.1) defines linear standing waves $\exp(\mathrm{i}\sigma_I t)\varphi_I(x, y, z)$, where $\mathrm{i}^2 = -1$. The natural sloshing modes φ_I should be regular and, generally speaking, analytically expandable over the mean free surface Σ_0 but, as is normal for linear fluid–structure interaction problems, the velocity potential can possess special asymptotic behaviour at the contact line l formed by $\Sigma_0 \cap S_0$.

As naturally occurs for axisymmetric tanks, the non-dimensional spectral boundary problem (2.1) divides into a family of spectral problems in the meridional plane, after introducing the cylindrical coordinate system (r, η, z) and separating the angular coordinate η by imposing

$$\varphi_I(r, \eta, z) = \begin{cases} \varphi_{m,n,c}(r, \eta, z), \\ \varphi_{m,n,s}(r, \eta, z) \end{cases}$$

$$= \phi_{mn}(r, z) \begin{cases} \cos(m\eta), \\ \sin(m\eta), \end{cases} \qquad m = 0, 1, \ldots, \quad n = 1, 2, \ldots, \tag{2.2}$$

and $\kappa_I = \kappa_{mn}$. Using (2.2) implies a composite index I, namely $I = (m, n, c)$ or $I = (m, n, s)$, where the non-negative integer $m \geqslant 0$ is associated with the angular wavenumber, $n \geqslant 1$ enumerates the natural modes within the same m, and c and s correspond to $\cos(m\eta)$ and $\sin(m\eta)$ components, respectively. Eigenfunctions $\phi_{mn}(r, z)$ come from the two-dimensional spectral boundary problem in domain G formed by

intersection of the mean liquid domain Q_0 and the meridional plane (see figure 1*b*):

$$\boxed{\frac{1}{r}\frac{\partial}{\partial r}\left(r\frac{\partial \phi_{mn}}{\partial r}\right)+\frac{\partial^2 \phi_{mn}}{\partial z^2}-\frac{m^2}{r^2}\phi_{mn}=0 \quad \text{in } G, \qquad \frac{\partial \phi_{mn}}{\partial n}=0 \quad \text{on } L} \tag{2.3}$$

$$\frac{\partial \phi_{mn}}{\partial z}=\kappa_{mn}\phi \quad \text{on } \Gamma, \tag{2.4}$$

where L and Γ are intersections of S_0 and Σ_0 with the meridional plane. In addition, the case $m=0$ requires the volume conservation condition

$$\int_0^{r_0} r\phi_{0n}\,\mathrm{d}r=0, \tag{2.5}$$

where r_0 is the radius of the circle Σ_0, $r_0=\sqrt{2h-h^2}$.

Faltinsen & Timokha (2012) constructed the Trefftz-type natural sloshing modes for a circular tank by treating the modes in terms of their analytical continuation into the 'air' area and an artificial normal velocity through the 'dry' tank surface yielded by this continuation. This Trefftz solution includes, in fact, two main components associated with two infinite harmonic functional sets. The first functional set is characterized by the zero normal artificial flow through the 'dry' tank surface, except at the tank top where it possesses a singular, multipole-type behaviour. In Faltinsen & Timokha (2012), the first component gave a dominant contribution to the natural sloshing modes for the non-dimensional liquid depths $0<h\lesssim 1.2$. The second functional set reflects the fact that analytical continuation of the natural sloshing modes can cause a non-zero Neumann trace on the 'dry' tank surface. The trace is assumed to be a continuous function, except at the tank top where it may have a jump. Because of the jump, the second component fell into two subclasses. The two subclasses gave a dominant contribution to the natural sloshing modes for the non-dimensional liquid depths $1.2\lesssim h<2$. Our aim is to generalize the results by Faltinsen & Timokha (2012) to the spherical tank shape by introducing two analogous functional sets, $\phi_j^{(m)}(r,z)$ and $\bar{\phi}_j^{(m)}(r,z)$, for the spectral problem (2.3)–(2.4).

2.2. *The first functional set, $\phi_i^{(m)}$*

An analogy of the first functional set by Faltinsen & Timokha (2010) (functions that satisfy the framed conditions (2.3) for arbitrary $0<h<2$) has been constructed by Barnyak *et al.* (2011). Based on this mathematical paper, we formulate an algorithm for computing (deriving) $\phi_i^{(m)}$ in supplementary material A (available at journals.cambridge.org/flm).

For the circular case, the first functional set admits a clear multipole-type treatment. A dipole-type component definitely exists for artificial flows associated with $\phi_i^{(m)}$ by Barnyak *et al.* (2011). For instance,

$$\phi_0^{(1)}(r,z)=\frac{2}{R^3}+\frac{1+R}{R(R-z+1)}, \qquad R=\sqrt{x^2+y^2+(z-1)^2}, \tag{2.6}$$

leads to the quantities $2\cos\eta/R^3$ and $2\sin\eta/R^3$ in the spatial representation by (2.2). The quantities determine a horizontal dipole along Ox or Oy, respectively, situated at the tank top. However, it is very difficult to extract the multipole-type components for other $\phi_i^{(m)}$ in the general case.

2.3. *The second functional set,* $\bar{\phi}_i^{(m)}$

The spherical domain admits a modified Poisson integral which can, for instance, be found in the handbook by Polyanin (2001, § 8.1.3-3) or in the paper by Dassios & Fokas (2008). If $W(x, y, z)$ is a harmonic function defined in the unit-radius spherical domain and $w_n = \partial W/\partial n$ is the continuous Neumann trace on $S_0 \cup \bar{S}_0$ (see figure 1*a*), the original function W is obtained from the trace w_n by the modified Poisson integral

$$W(x, y, z) = \frac{1}{4\pi} \int_{S_0 \cup \bar{S}_0} \underbrace{\left[-\frac{2}{R} + \ln(R - F) \right]}_{\mathscr{G}_s(P;\boldsymbol{P}_*)} w_n(\boldsymbol{P}_*)\, \mathrm{d}S(\boldsymbol{P}_*), \tag{2.7}$$

where $\boldsymbol{P} = (x, y, z)$ is the radius vector of an arbitrary point inside the sphere, $\boldsymbol{P}_* = (x_*, y_*, z_*)$ is the radius vector of a point on the spherical surface, $R = \|\boldsymbol{P} - \boldsymbol{P}_*\|$ is the distance between these points, and $F = (\boldsymbol{P} - \boldsymbol{P}_*) \cdot \boldsymbol{P}_* = \boldsymbol{P} \cdot \boldsymbol{P}_* - 1 \leqslant 0$ is the projection of $\boldsymbol{P}$ on the outer normal vector to the sphere at the point $\boldsymbol{P}_*$. The Neumann trace w_n should also satisfy the necessary condition

$$\int_{S_0 \cup \bar{S}_0} w_n \, \mathrm{d}S = 0, \tag{2.8}$$

implying mass conservation.

Based on (2.7), we define the second functional set $\bar{\phi}_i^{(m)}$ that, in contrast to $\phi_j^{(m)}$, can have a non-zero Neumann trace on the 'dry' surface $\bar{S}_0$. Introducing the spherical coordinate system for points $\boldsymbol{P}_* = (\sin\theta\cos\varphi, \sin\theta\sin\varphi, \cos\theta)$ belonging to $\bar{S}_0$ leads to

$$\mathscr{G}_s = \mathscr{G}_s(x, y, z; \theta, \varphi), \quad w_n = w_n(\theta, \varphi) \quad \text{on } \bar{S}_0 \quad \text{and} \quad w_n = 0 \quad \text{on } S_0, \tag{2.9}$$

where $w_n(\theta, \varphi)$ is a 2π-periodic function with respect to φ that can be represented by the Fourier series

$$w_n(\theta, \varphi) = \sum_{m=0}^{\infty} f_m \cos(m(\varphi - \varphi_{\theta m}))\, v_m(\theta), \quad 0 < \theta < \theta_0, \, 0 \leqslant \varphi < 2\pi \tag{2.10}$$

with appropriate coefficients f_m, phase shifts $\varphi_{\theta m}$, and functions $v_m(\theta)$. Condition (2.8) reads as

$$\int_0^{\theta_0} \sin\theta \, v_0(\theta) \, \mathrm{d}\theta = 0 \quad \text{and, in addition,} \quad v_m(\theta_0) = 0, \quad m = 0, 1, \ldots. \tag{2.11}$$

The latter condition at $\theta = \theta_0$ follows from results by Komarenko (Lukovsky *et al.* 1984; Komarenko 1998, §13) requiring the continuous function w_n to be zero on the contact line between S_0 and $\bar{S}_0$ for the spectral boundary problem (2.1).

After substituting (2.10) into (2.7) and using the cylindrical coordinates (r, η, z) instead of (x, y, z), a tedious derivation makes it possible to separate the angular coordinate η and arrive at the integral representation of the (r, z)-function satisfying the framed conditions (2.3):

$$\bar{\phi}_j^{(m)}(r, z) = \frac{1}{4\pi} \int_0^{\theta_0} \int_0^{2\pi} \left[-\frac{2}{R_\tau} + \ln(R_\tau - F_\tau) \right] \times \cos(m\tau) \, \mathrm{d}\tau \underbrace{\sin\theta \, v_{mj}(\theta)}_{\nu_{mj}(\theta)} \mathrm{d}\theta, \quad m \geqslant 0. \tag{2.12}$$

Here

$$\left.\begin{aligned} R_\tau &= \sqrt{r^2+\sin^2\theta-2r\sin\theta\cos\tau+(z-\cos\theta)^2},\\ F_\tau &= r\sin\theta\cos\tau+z\cos\theta-1\leqslant 0 \end{aligned}\right\} \tag{2.13}$$

and $\mathscr{V}_{mj}(\theta)$, $j\geqslant 1$, is an arbitrary function on the interval $[0,\theta_0]$ that satisfies the condition

$$\int_0^{\theta_0}\mathscr{V}_{0j}(\theta)\,\mathrm{d}\theta=0 \quad\text{and}\quad \mathscr{V}_{mj}(\theta_0)=0, \quad \text{for } m=0,1,\ldots. \tag{2.14}$$

Additional information on $\mathscr{V}_{mj}(\theta)$ at $\theta=0$ follows from analytical continuation of $\partial\phi_{mn}/\partial z$ from G up to the tank top. For $m=0$, this derivative is an even function with respect to r at $r=0$, but $m\neq 0$ causes the partial derivative to be an odd function with respect to r. This implies that $\mathscr{V}_{mj}(\theta)$ should be an odd function with respect to θ for $m=0$ and an even function for $m\neq 0$. One should note that the continuity of $\mathscr{V}_{mj}(\theta)$, $j\geqslant 1$ at $\theta=0$ does not mean that the related Neumann trace is finite and continuous at $\theta=0$ (tank top). For circular tanks, such a discontinuity at the tank top has yielded two subclasses of functions.

When $\mathscr{V}_{mj}(\theta)$, $j\geqslant 1$ is a complete system of functions on $[0,\theta_0]$ satisfying (2.14) and possessing the odd/even features at $\theta=0$, integral representation (2.12) yields the required harmonic functional set $\bar{\phi}_j^{(m)}(r,z)$. In the present paper, we involve the Legendre polynomials $\mathrm{P}_i(.)$ for $\mathscr{V}_{mj}(\theta)$, $j\geqslant 1$ by postulating

$$\mathscr{V}_{mj}(\theta)=(z_0^2-\cos^2\theta)\mathrm{P}_{2j-2}\left(\frac{\theta}{\theta_0}\right), \tag{2.15}$$

for $j\geqslant 1$ and $m\geqslant 1$, and

$$\left.\begin{aligned} \mathscr{V}_{mj}(\theta) &= (z_0^2-\cos^2\theta)\left[\mathrm{P}_{2j+1}\left(\frac{\theta}{\theta_0}\right)-\frac{b_i}{b_0}\frac{\theta}{\theta_0}\right],\\ b_i &= \int_0^{\theta_0}(z_0^2-\cos^2\theta)\mathrm{P}_{2i+1}\left(\frac{\theta}{\theta_0}\right)\mathrm{d}\theta, \end{aligned}\right\} \tag{2.16}$$

for $j\geqslant 1$ and $m=0$. Supplementary material B presents computational details.

3. Numerical results: approximate κ_{mn} and ϕ_{mj}

3.1. *The Trefftz solution based on combining $\phi_j^{(m)}$ and $\bar{\phi}_j^{(m)}$*

Employing $\phi_j^{(m)}$ and $\bar{\phi}_j^{(m)}$ defines the Trefftz solution

$$\phi_{mn}(r,z)=\sum_{i=1}^{q_1}c_i\phi_{i-1}^{(m)}(r,z)+\sum_{i=q_1+1}^{q_1+q_2}c_i\bar{\phi}_{i-q_1}^{(m)}(r,z)=\sum_{k=1}^{q_1+q_2}c_i\Phi_i^{(m)}(r,z) \tag{3.1}$$

of the spectral problem (2.3)–(2.4), which exactly satisfies the framed condition (2.3) and, in addition, defines an analytical continuation of ϕ_{mn} across the mean free surface into the 'air' area. Coefficients c_i and corresponding eigenvalues κ_{mn} should follow from the non-framed condition (2.4), which is equivalent to the variational equation

$$\int_0^{r_0}r\Phi_i^{(m)}(r,z_0)\left(\frac{\partial\phi_{mn}}{\partial z}(r,z_0)-\kappa_{mn}\phi_{mn}(r,z_0)\right)\mathrm{d}r=0, \quad i=1,\ldots,q_1+q_2. \tag{3.2}$$

Substituting (3.1) into (3.2) leads to the spectral matrix problem $(\boldsymbol{A} - \kappa_{mn}\boldsymbol{B})\boldsymbol{c} = 0$, where

$$\left.\begin{aligned} \boldsymbol{A} &= \{a_{ij}\}, \quad a_{ij} = \int_0^{r_0} r \frac{\partial \Phi_i^{(m)}}{\partial z}(r, z_0)\Phi_j^{(m)}(r, z_0)\,\mathrm{d}r, \\ \boldsymbol{B} &= \{b_{ij}\}, \quad b_{ij} = \int_0^{r_0} r\Phi_i^{(m)}(r, z_0)\Phi_j^{(m)}(r, z_0)\,\mathrm{d}r. \end{aligned}\right\} \tag{3.3}$$

We cannot prove it, but each functional set $\{\phi_j^{(m)}(r, z_0), j \geqslant 0\}$ and $\{\bar{\phi}_j^{(m)}(r, z_0), j \geqslant 1\}$ is, most probably, a complete basis on the interval $[0, r_0]$ for any fixed m. This can be numerically dangerous. Increasing both q_1 and q_2 leads to ill-posed matrices $\boldsymbol{A}$ and $\boldsymbol{B}$. The same problem was discussed by Faltinsen & Timokha (2010). Its solution requires that at least one of the numbers q_i, $i = 1, 2$ should not be large.

A non-optimized FORTRAN code was written in double precision (16 digits) to test applicability of the Trefftz solution (3.1).

3.2. *Eigenvalues and natural sloshing modes*

The Trefftz solution (3.1) provides rapid convergence to eigenvalues κ_{mn} for $0 < h < 1.99$. Normally, $8 < q_1 + q_2 < 20$ leads to stabilization of six significant figures in the numerical eigenvalues κ_{mi}, $i = 1, \ldots, 6$. The eigenvalues are fully consistent with the numerical results of McIver (1989) for nine different liquid depths from 0.2 to 1.8 and $\{\kappa_{mi} : i = 1, 2, 3, 4,\ m = 0, 1, 2, 3\}$ reported by McIver. Suggesting that this can be useful in practice, we present the numerical eigenvalues $\{\kappa_{mi} : i = 1, \ldots, 6,\ m = 0, \ldots, 5\}$ in the tables of the supplementary material.

The actual numbers q_1 and q_2 used in our calculations were different for different liquid depths. For lower liquid depths, $0 < h \lesssim 0.5$, we can neglect the contribution of $\bar{\phi}_j^{(m)}$ and thereby obtain the solution of Barnyak *et al.* (2011). In the range $0.5 \lesssim h \lesssim 0.8$, a few functions (one or two) $\bar{\phi}_j^{(m)}(r, z_0)$ should be taken to accelerate convergence with increasing q_1. An approximately half-filled tank with $0.8 \lesssim h \lesssim 1.2$ requires four or five functions $\phi_j^{(m)}$ and four to six functions $\bar{\phi}_j^{(m)}$ to get numerical results in the aforementioned tables. Increasing liquid depth to $1.2 \lesssim h \lesssim 1.9$ needs more basic functions $\bar{\phi}_j^{(m)}$ (normally 10–16) and only a few (one or two) functions $\phi_j^{(m)}$ for obtaining six significant figures of κ_{mi}, $i = 1, \ldots, 6$. Finally, the eigenvalues for an almost filled tank, $1.9 \lesssim h \leqslant 1.99$, can be computed without the functions $\phi_j^{(m)}$. Computations with $1.99 < h$ were often numerically unstable due to decreasing interval $[0, r_0]$ in (3.3). The instability can probably be avoided via an appropriate normalization in the codes.

The numerical values $(r_0\kappa_{mi})$ at $h = 1.99$ can be considered as an approximation of the so-called 'ice-fishing' problem with a circular hole (Kozlov & Kuznetsov 2004): $\tilde{\kappa}_{mn} = \lim_{h\to 2}(\kappa_{mn}r_0)$. The numerical values $\tilde{\kappa}_{mn}$ were reported by McIver (1989) for $m = 0, 1, 2, 3$ and $n = 1, 2, 3, 4$. Our approximate eigenvalues $(r_0\kappa_{0i})$, $i = 1, \ldots, 4$ with $h = 1.99$ are equal to 4.098, 7.309, 10.48, 13.63, which generally agrees with the $\tilde{\kappa}_{0i}$, $i = 1, \ldots, 4$ of McIver (1989), equal to 4.1213, 7.34208, 10.51708, 13.6773. Furthermore, our numerical values $(r_0\kappa_{1i})$, $i = 1, \ldots, 4$ for $h = 1.99$ are 2.678, 5.833, 8.977 and 12.12, but $\tilde{\kappa}_{1i}$, $i = 1, \ldots, 4$ of McIver (1989) are equal to 2.75476, 5.89215, 9.03285 and 12.1741; $(r_0\kappa_{2i})$, $i = 1, \ldots, 4$ for $h = 1.99$ are 4.052, 7.282, 10.46 and 13.62, while the limiting values are 4.1213, 7.34208, 10.51708 and 13.6773; and $(r_0\kappa_{3i})$, $i = 1, \ldots, 4$ for $h = 1.99$ are 5.332, 8.656, 11.88 and 15.07, with $\tilde{\kappa}_{0i}$, $i = 1, \ldots, 4$ by McIver (1989) equal to 5.400, 8.71829, 11.94062 and 15.1293.

Because the natural sloshing modes are defined to within a multiplier, the normalization

$$\int_0^{r_0} r\phi_{mi}(r, z_0)\,\mathrm{d}r = 1, \quad \phi_{mi}(r, z) := \frac{\phi_{mi}(r, z)}{\mathrm{sgn}\,(\phi_{mi}(r_0, z_0))} \tag{3.4}$$

was used, imposing, in particular, a positive vertical elevation at the wall. The sign ':=' means the same as in some programming languages, i.e. one should substitute ϕ_{mi} in the right-hand side to get the final expression in the left-hand side. Convergence of the Trefftz solution (3.1) to the natural sloshing modes is quite rapid. Because the framed conditions of (2.3) are exactly fulfilled, the convergence should be uniquely established for the non-framed (spectral) condition on L. In the cases when the six to eight significant figures of κ_{mi}, $i = 1, \ldots, 6$ are stabilized, this solution normally stabilizes three or four significant figures of the approximate radial surface profiles $f_{mi}(r) = \phi_{mi}(r, z_0)$ in the uniform metrics. Provided by normalization (3.4), the mean square error $\epsilon_{mi} = \sqrt{\int_0^{r_0} (\partial\phi_{mi}/\partial x(r, z_0) - \kappa_{mi}\phi_{mi}(r, z_0))^2\,\mathrm{d}r}$ was established to be in the range between 10^{-2} and 10^{-4}.

Using our approximate natural sloshing modes, one can discover how the radial surface wave profiles, $f_{mi}(r) = \phi_{mi}(r, z_0)$, change with the liquid depth. The results are illustrated in figure 2 for the four lower modes with $m = 1$. We remark that, when $0 < h \lesssim 0.5$, the radial surface wave profile for the lowest natural sloshing modes related to ϕ_{11} becomes close to a linear function, i.e. $\phi_{11}(r, z_0) \approx Cr$, where C is a constant. Bearing in mind the corresponding three-dimensional wave patterns, we find $f_{11}(r)\cos\eta \approx Cr\cos\eta = Cx$ and $f_{11}(r)\sin\eta \approx Cr\sin\eta = Cy$, whose linear combination determines an inclination of an almost flat free surface. Furthermore, recalling that the natural sloshing modes are orthogonal on Σ_0 and the forcing terms due to a horizontal tank excitation are proportional to the hydrodynamic coefficients (see (5.26) in Faltinsen & Timokha 2009)

$$\lambda_n = \pi \int_0^{r_0} r^2 f_{1n}(r)\,\mathrm{d}r, \quad n \geqslant 1, \tag{3.5}$$

we see that (i) the forced linear sloshing in a spherical tank with $0 < h \lesssim 0.5$ is uniquely associated with the first (lowest) natural sloshing modes, and (ii) these lowest modes define spatial wave patterns which look like an inclination of an almost flat free surface. The appearance of other, complex wave patterns means that the free-surface nonlinearity and/or initial perturbations of higher modes matter.

Increasing liquid depth yields more complicated radial free surface profiles. Figure 2 shows that when $1 < h < 2$ there are no local extrema at the wall as expected for upright cylindrical tanks. This addresses the so-called 'high spots' (the points on the mean free surface, where its elevation attains the maximum and minimum values) problem for the spherical tank shape. Kulczycki & Kuznetsov (2011) proved the corresponding theorems for the two-dimensional sloshing problem that are illustrated by Faltinsen & Timokha (2010) for a circular tank.

4. Conclusions

After reporting the Trefftz solution for a two-dimensional sloshing problem in a circular tank (Faltinsen & Timokha 2012), we asked the natural question whether an analogous solution is possible for spherical tanks.

The solution of Faltinsen & Timokha (2012) contains two different special analytical components treated in terms of analytical continuation of the natural sloshing modes to

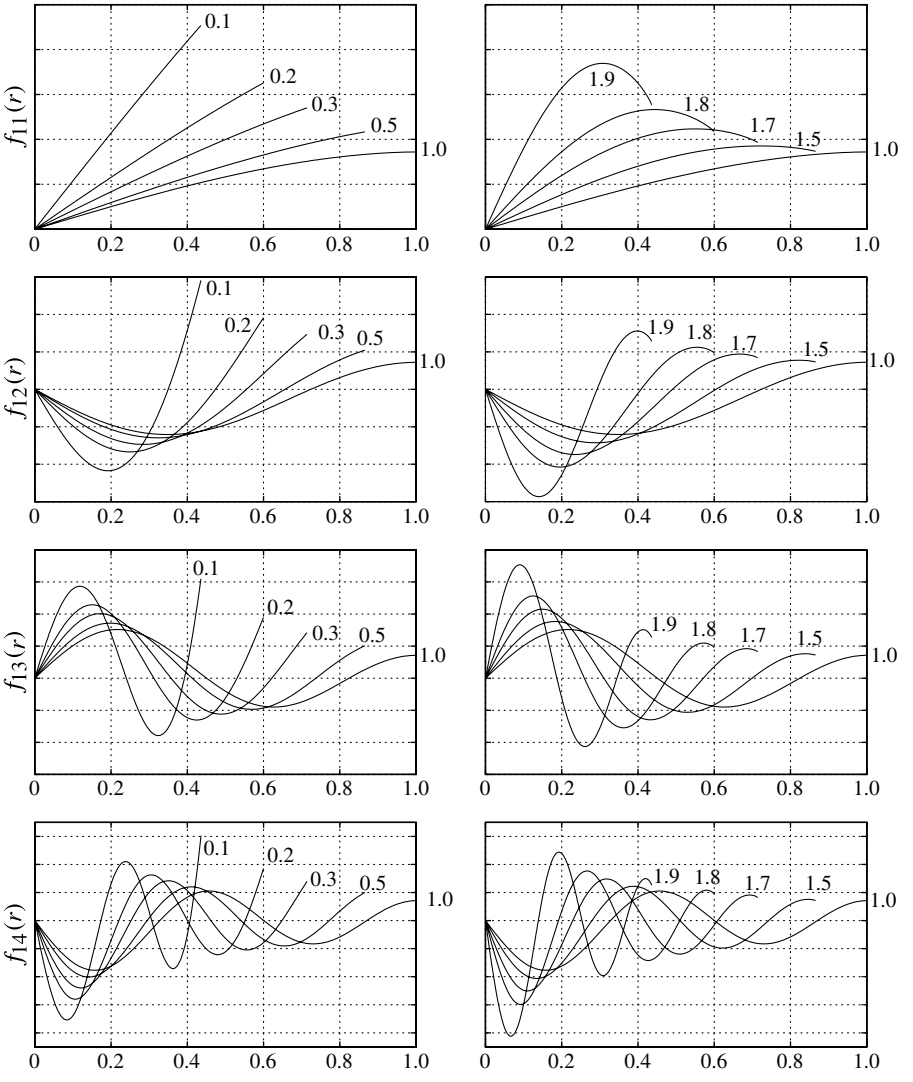

FIGURE 2. The radial wave profiles, $f_{1i}(r) = \phi_{1i}(r, z_0)$, $i = 1, \ldots, 4$, for different non-dimensional liquid depths. The labels of the graphs mark the depths. The figure demonstrates that 'high spots' are not at the walls for $1 < h < 2$. Further, the surface wave patterns of the two lowest natural sloshing modes are for $0 < h \lesssim 0.5$ close to an inclined flat plane provided by $f_{11}(r)\cos\eta \approx Cr\cos\eta = Cx$ and $f_{11}(r)\sin\eta \approx Cr\sin\eta = Cy$, where C is a constant.

the 'air' domain. One difficulty is that, even though Barnyak *et al.* (2011) constructed an analogy of the first 'singular' component, the functional set arising from this paper cannot be related to spatial multipoles, and therefore the derivation scheme by Faltinsen & Timokha (2012), employing an assumption on continuously distributed multipoles on the 'dry' tank surface, generally fails. However, we can continue treating the second component as giving a non-zero artificial normal flow through the 'dry' wall and represent it by using the modified Poisson integral (Dassios & Fokas 2008) with a continuous (except at the tank top) Neumann trace. This action leads to the

required second set of functions. The constructed Trefftz solution shows a rapid convergence to both natural sloshing modes and frequencies.

Based on the constructed Trefftz approximation, we were able to establish specific properties of the linear sloshing solution. For lower liquid depths, $0 < h \lesssim 0.5$, we see that: (i) analytical continuation of the velocity potential is characterized by almost zero artificial flow through the 'dry' wall except at the tank top, where a strong singular behaviour occurs, (ii) instant steady-state wave patterns occurring due to horizontal tank excitation look like an inclination of an almost flat free surface, and (iii) complicated wave patterns are uniquely caused by the free-surface nonlinearity and/or initial perturbations of higher modes. The higher modes cannot be directly excited by a harmonic horizontal tank forcing. For higher liquid depths, $1 < h < 2$, our analysis demonstrates that (i) an artificial normal liquid flow through the 'dry' tank surface (caused by the analytical continuation) becomes far from zero, (ii) the 'high spots', the points on the mean free surface where its elevation attains the maximum and minimum values, are not at the wall, which is in agreement with the assertion proved by Kulczycki & Kwaśnicki (2012).

Supplementary material

Supplementary movies are available at journals.cambridge.org/flm.

REFERENCES

BARNYAK, M., GAVRILYUK, I., HERMANN, M. & TIMOKHA, A. 2011 Analytical velocity potentials in cells with a rigid spherical wall. *Z. Angew. Math. Mech.* **91** (1), 38–45.

BUDIANSKY, B. 1958 Sloshing of liquids in circular canals and spherical tanks. *Tech. Rep.* Lockheed Aircraft Corporation, Missile System Division, Sunnyvale, California.

BUDIANSKY, B. 1960 Sloshing of liquid in circular canals and spherical tanks. *J. Aerosp. Sci.* **27** (3), 161–172.

CURADELLI, O., AMBROSINI, D., MIRASSO, A. & AMANI, M. 2010 Resonant frequencies in an elevated spherical container partially filled with water: FEM and measurement. *J. Fluids Struct.* **26** (1), 148–159.

DASSIOS, G. & FOKAS, A. S. 2008 Methods for solving elliptic PDSs in spherical coordinates. *SIAM J. Appl. Math.* **68**, 1080–1096.

DRODOS, G. C., DIMAS, A. A. & KARABALIS, D. L. 2008 Discrete modes for seismic analysis of liquid storage tanks of arbitrary shape and height. *J. Pressure Vessel Technology* **130**, 0418011.

FALTINSEN, O. M. & TIMOKHA, A. N. 2009 *Sloshing*. Cambridge University Press.

FALTINSEN, O. M. & TIMOKHA, A. N. 2010 A multimodal method for liquid sloshing in a two-dimensional circular tank. *J. Fluid Mech.* **665**, 457–479.

FALTINSEN, O. M. & TIMOKHA, A. N. 2012 On sloshing modes in a circular tank. *J. Fluid Mech.* **695**, 467–477.

KARAMANOS, S. A., PAPAPROKOPIOU, D. & PLATYRRACHOS, M. A. 2006 Sloshing effects on the seismic design of horizontal–cylindrical and spherical industrial vessels. *J. Pressure Vessel Technology* **128**, 328–340.

KARAMANOS, S. A., PAPAPROKOPIOU, D. & PLATYRRACHOS, M. A. 2009 Finite element analysis of externally-induced sloshing in horizontal–cylindrical and axisymmetric liquid vessels. *J. Pressure Vessel Technology* **131** (5), Paper No. 051301.

KOMARENKO, A. 1980 Asymptotic expansion of eigenfunctions of a problem with a parameter in the boundary conditions in a neighborhood of angular boundary points. *Ukrainian Math. J.* **32** (5), 433–437.

KOMARENKO, A. 1998 Asymptotics of solutions of spectral problems of hydrodynamics in the neighborhood of angular points. *Ukrainian Math. J.* **50** (6), 912–921.

KONDRATIEV, V. 1967 Boundary problems for elliptic equations in domains with conical or angular points. *Trans. Moscow Math. Soc.* **16**, 227–313.

KOZLOV, V. & KUZNETSOV, N. 2004 The ice-fishing problem: the fundamental sloshing frequency versus geometry of holes. *Math. Meth. Appl. Sci.* **27**, 289–312.

KULCZYCKI, T. & KUZNETSOV, N. 2011 On the high spots of fundamental sloshing modes in a trough. *Proc. R. Soc.* A **467** (2132), 2427–2430.

KULCZYCKI, T. & KWAŚNICKI, M. 2012 On high spots of the fundamental sloshing eigenfunctions in axially symmetric domains. *Proc. Lond. Math. Soc.*, in press.

LAMB, H. 1932 *Hydrodynamics*. Cambridge University Press.

LUKOVSKY, I. A., BARNYAK, M. Y. & KOMARENKO, A. N. 1984 *Approximate Methods of Solving the Problems of the Dynamics of a Limited Liquid Volume*. Naukova Dumka (in Russian).

MCIVER, P. 1989 Sloshing frequencies for cylindrical and spherical containers filled to an arbitrary depth. *J. Fluid Mech.* **201**, 243–257.

PATKAS, L. & KARAMANOS, S. A. 2007 Variational solution of externally induced sloshing in horizontal–cylindrical and spherical vessels. *J. Engng Mech.* **133** (6), 641–655.

POLYANIN, A. D. 2001 *Handbook of Linear Partial Differential Equations for Engineers and Scientists*. Chapman and Hall/CRC.

REBOUILLAT, S. & LIKSONOV, D. 2010 Fluid–structure interaction in partially filled liquid containers: a comparative review of numerical approaches. *Comput. Fluids* **39**, 739–746.